IEEE Photonics Journal
An IEEE Photonics Society Publication

Open Access

Experimental Evidence of the Impact of Nitrogen on Carrier Capture and Escape Times in InGaAsN/GaAs Single Quantum Well

Volume 4, Number 6, December 2012

Lifang Xu
Dinesh Patel
Carmen S. Menoni, Fellow, IEEE
Jeng-Ya Yeh
Luke J. Mawst, Fellow, IEEE
Nelson Tansu, Senior Member, IEEE

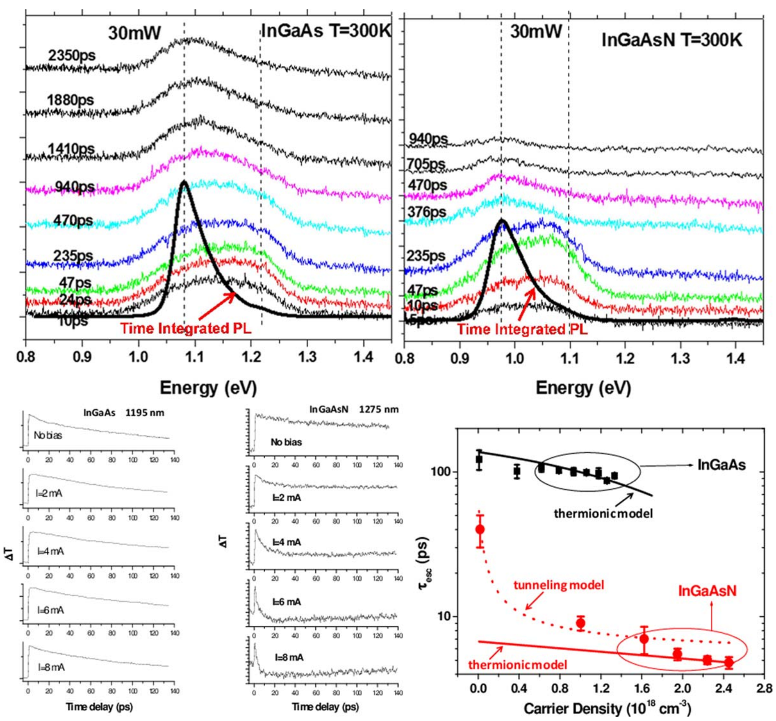

DOI: 10.1109/JPHOT.2012.2230251
1943-0655/$31.00 ©2012 IEEE

IEEE photonics SOCIETY

IEEE

Experimental Evidence of the Impact of Nitrogen on Carrier Capture and Escape Times in InGaAsN/GaAs Single Quantum Well

Lifang Xu,[1] Dinesh Patel,[1] Carmen S. Menoni,[1] *Fellow, IEEE*, Jeng-Ya Yeh,[2] Luke J. Mawst,[2] *Fellow, IEEE*, and Nelson Tansu,[3] *Senior Member, IEEE*

[1]Department of Electrical and Computer Engineering, Colorado State University, Fort Collins, CO 80523 USA
[2]Reed Center for Photonics, Department of Electrical and Computer Engineering, University of Wisconsin-Madison, Madison, WI 53706 USA
[3]Center for Photonics and Nanoelectronics, Department of Electrical and Computer Engineering, Lehigh University, Bethlehem, PA 18015 USA

DOI: 10.1109/JPHOT.2012.2230251
1943-0655/$31.00 ©2012 IEEE

Manuscript received October 15, 2012; revised November 20, 2012; accepted November 22, 2012. Date of publication November 29, 2012; date of current version December 7, 2012. This work was supported in part by the U.S. National Science Foundation under Grants ECCS 03134410 and ECCS 1028490 and in part by the Class of 1961 Professorship (N.T.). Corresponding authors: N. Tansu, L. Xu, C. S. Menoni, and L. J. Mawst (e-mail: tansu@lehigh.edu; lifangxu417@yahoo.com; carmen.menoni@colostate.edu; mawst@engr.wisc.edu).

Abstract: We report our experimental results and theoretical analysis on carrier escape time in $In_{0.4}Ga_{0.6}As_{1-y}N_y/GaAs$ ($y = 0$; 0.005) ridge waveguide single-quantum-well (QW) lasers with N-contents of 0% and 0.5%. The experiments were carried out by using novel time-resolved two-color pump–probe transmission measurements. Our results show a significant decrease of carrier escape time with nitrogen incorporation in the InGaAsN QW, which agrees well with the values obtained from the theoretical calculation based on thermally activated hole leakage. The measurement results provide experimental supports for hole leakage theory.

Index Terms: Quantum-well (QW) lasers, carrier capture and escape process, InGaAsN, 1.3-μm lasers.

1. Introduction

Dilute-nitride-based diode lasers have significant applications for uncooled telecom applications [1]–[9]. Significant progress has been realized resulting in low-threshold diode lasers operating at 1300–1500 nm for dilute-nitride-based active regions [1]–[14], resulting in low-temperature-sensitive lasers operating at this spectral regime. Several studies have been attempted to understand the dominant factors limiting the temperature sensitivity [10]–[14] and optical gain and threshold characteristics [15]–[23] of dilute-nitride lasers.

Recently, high-performance InGaAsN/GaAs quantum-well (QW) lasers have been demonstrated with high-speed modulation bandwidth [24], [25]. However, these benchmarks are still distanced from the high-frequency bandwidth limit predicted by theories [26], [27]. The carriers capture (τ_{cap}) and escape times (τ_{esc}) are very important parameters that determine the static and dynamic performances of QW lasers [28]–[30]. In dynamic operating conditions, the capture and escape times affect both the resonant frequency and the damping rate of the modulation response [28]–[30], and thus determine the modulation bandwidth of the lasers.

It has been pointed out that the bandwidth of current dilute-nitride lasers are mainly limited by thermal effects that reduce the effective differential gain and lead to a rapid increase of the threshold current and reduction of external differential quantum efficiency [31], [32]. In addition, supportive theoretical calculations of carrier thermionic escape process have suggested the existence of an increased hole leakage, as a contributing factor to the device temperature sensitivity [33]. However, no direct experimental evidence on the hole leakage effect in InGaAsN QW laser has been provided so far. These calculations have relied on the assumption of a smaller valence-band offset in the InGaAsN QW lasers [33], which also contains significant uncertainty from experiments. Motivated by this necessity, in this paper, we investigate the carrier capture and escape processes (τ_{cap} and τ_{esc}) of InGaAsN/GaAs QW lasers under different biasing conditions, at room temperature, by using a novel two-color pump–probe differential transmission measurements and time-resolved photoluminescence (TRPL) measurement. An identical laser structure with identical In-content InGaAs QW without any nitrogen incorporation is also measured as control sample.

From the experimental results, τ_{esc} with bias current for the InGaAsN QW laser show a different trend, and τ_{esc} for InGaAsN QW lasers are one order of magnitude smaller in comparison with those measured of InGaAs QW laser at higher current. The dependence of τ_{esc} on carrier density in dilute-nitride QW lasers for low-carrier-density operation is only explained if tunneling through the triangular-biased QW is considered. However, the behavior of τ_{esc} on carrier density in InGaAsN QW lasers at high carrier density can be explained well with the thermionic carrier escape model. The tunneling mechanism is most important at low carrier densities, as expected for a smaller band offset ratio. In contrast, the τ_{esc} characteristics of the InGaAs QW laser can be well explained by the thermionic carrier escape model for the wide range of carrier density investigated here.

2. Experimental Works

The carrier escape and capture processes were investigated on two identical $In_{0.4}Ga_{0.6}As$ and $In_{0.4}Ga_{0.6}As_{0.995}N_{0.005}$ single-QW ridge waveguide (RWG) lasers. Both of the lasers were grown on GaAs substrates by low-pressure (200 mbar) and low-temperature (530 °C) metal–organic chemical vapor deposition (MOCVD), with the details of the growths provided in reference [34]. The two device structures consist of a 6-nm single-QW active layer sandwiched by two tensile strain $GaAs_{0.85}P_{0.15}$ barriers, a 300-nm GaAs separate confinement region (SCH), and AlGaAs claddings. The uncoated RWG InGaAsN (InGaAs) devices feature a stripe width of 3.5 μm and a cavity length of 500 μm, with emission wavelengths of $\lambda = 1275$ nm (1195 nm). The threshold current at room temperature were measured to be $I_{th} = 18$ mA (10 mA).

All previously reported two-color pump–probe transmission measurements required a high-power laser oscillator to generate a broadband continuum to serve as probe beam other than pump laser beam [35]–[37]. Aside from the experimental difficulty, such high power was prone to disturb the equilibrium of the measured system and make the data interpretation more challenging.

Here, instead, as shown in Fig. 1, we utilized residue light from a 800-nm mode-locked Ti-sapphire pulse laser as pump beam, and the probe pulse train was generated from an optical parametric oscillator (OPO), which was synchronously pumped by the mode-locked Ti-sapphire pulse laser, which, for the first time, allow direct measurement of carrier capture and escape processes in InGaAsN/GaAs QW structures. The Ti-sapphire oscillator emitted 100-fs pulses centered at a wavelength of 800 nm with 82-MHz repetition rate and average power of 900 mW. The average output power of the OPO was about 40 mW, with a pulsewidth of 150 fs. The wavelength of the OPO was tuned to the corresponding emission wavelengths of the laser devices under study, i.e., 1280 nm for InGaAsN QW lasers and 1200 nm for InGaAs QW lasers, respectively. Using an ND filter, the power of the pump beam was chosen to be around 3 mW and ten times larger than that of the probe beam. Relative delay between the pump and the probe was controlled through a stepping-motor-driven translation stage. Two microscope objectives were used to couple light in and out of the

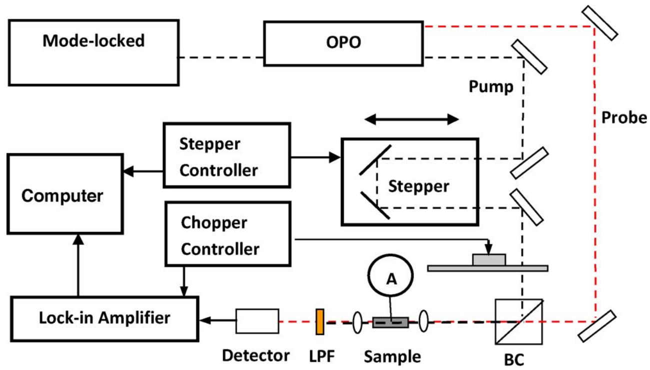

Fig. 1. Experimental set up for two-color pump–probe transmission measurements. BC: beam combiner. A: current source.

waveguide of the RWG laser devices. Taking advantage of the different wavelengths of the pump and the probe, we eliminated the pump pulses by using a 1150-nm long-pass filter (LPF) before the final detection, and the change in probe transmission were detected as a function of pump–probe delay. Here, the lock-in technique was used, where only pump beam was chopped and the probe beam was measured at chopper frequency.

The carrier transport and carrier capture processes were investigated through the temporal evolutions of photoluminescence (PL), which employed a luminescence upconversion setup. The detail of the temporal evolution PL setup was described in our previous works [38].

3. Results and Discussion—Analysis

Fig. 2 shows the change of probe transmission, i.e., ΔT, induced by the pump as a function of pump–probe delay with different biasing conditions. An exponential decay following an instantaneous rise was observed for both lasers (see Fig. 2), and the carrier lifetimes were fitted following an exponential relation of $\Delta T = \Delta T_0 \times \exp(-t/\tau)$. With the pump beam exciting only the unconfined state outside of the QW and probing the ground state in the well, the rise time of ΔT reflects the process of carrier capture into the well. The decay time can be ascribed to contribution of both carrier escape from the well and carrier recombination. The latter, from our results of PL lifetime measurements at room temperature, is on the order of 300–400 ps for InGaAsN and >2 ns for InGaAs lasers, respectively, as shown in the TRPL spectra comparison of $In_{0.4}Ga_{0.6}As_{0.995}N_{0.005}$ QW and $In_{0.4}Ga_{0.6}As$ QW samples performed at $T = 300$ K (see Fig. 3) with carrier density of n $\sim 2 \times 10^{18}$ cm^{-3}. Note that the carrier recombination lifetimes in the QW include the contribution from both the radiative and nonradiative (Auger and monomolecular) recombination processes, and these total carrier lifetimes are relatively long in comparison with the decay rate of ΔT from the probe transmission measurements. The Auger process is a strong carrier-dependent process for high-carrier-density operation near threshold conditions; however, the total carrier lifetimes are found to be an order of magnitude larger in comparison with the decay rate ΔT. Thus, the decay of ΔT observed here mainly represents the carrier escape dynamics. Note that the samples were not biased in the TRPL measurements and the escape process was highly dependent on carrier density in the QW. In our TRPL measurements, the measured carrier lifetime is a combination of both the radiative and nonradiative recombination processes, as well as possible escape processes. In the pump–probe experiments, the device was biased with a perturbation introduced from the pump beam, which led to the probe revealing the differential carrier lifetimes. Previous data on the strong dependence of the external differential quantum efficiency with temperature is indicative of carrier leakage [10], [13], [39], since Auger recombination should only impact the temperature dependence of the threshold current [16].

A more significant decrease of decay time with increased bias can be observed for the dilute-nitride laser, compared with the InGaAs laser. At a bias just below threshold, τ_{esc} is found to be one

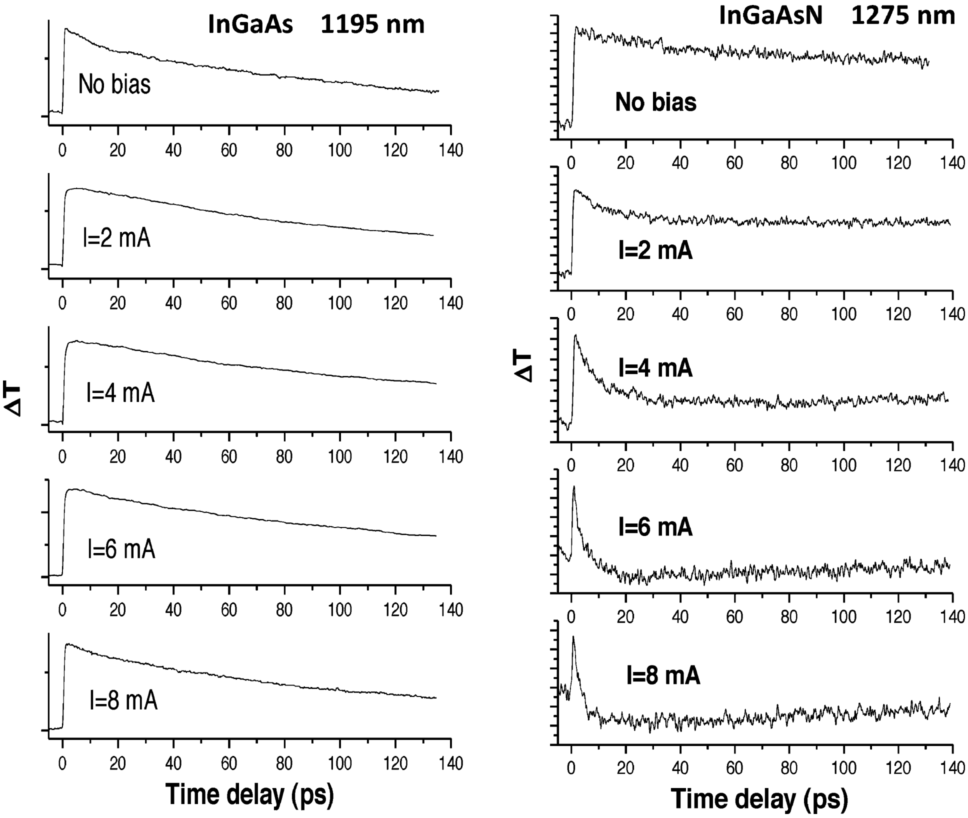

Fig. 2. Relative changes in the probe transmission induced by the pump as a function of the pump–probe delay, for both InGaAs and InGaAsN RWG lasers. The biasing is varied below threshold. The traces are recorded at the wavelengths indicated in the figure.

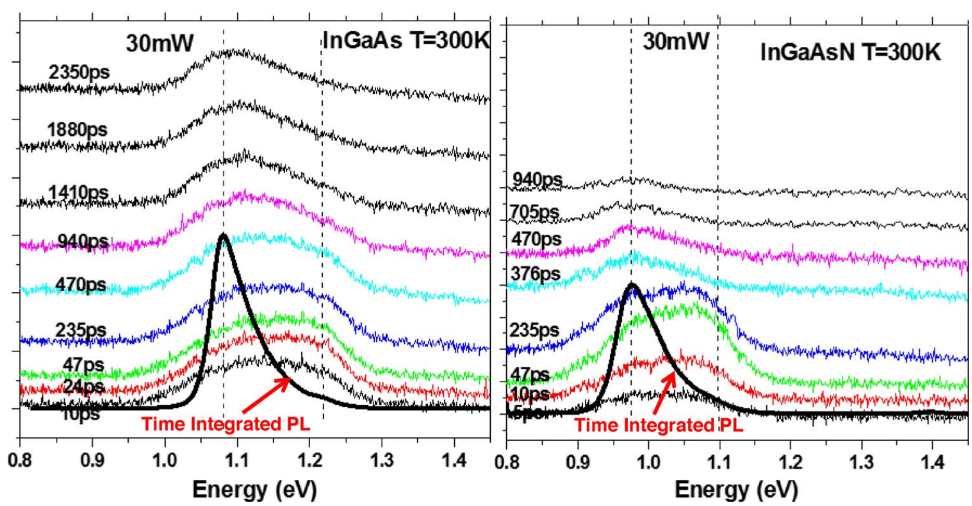

Fig. 3. TRPL spectra at $T = 300$ K for $In_{0.4}Ga_{0.6}As_{0.995}N_{0.005}$ QW and $In_{0.4}Ga_{0.6}As$ QW samples. The solid black traces with arrows are time integrated PL spectra.

order of magnitude lower in InGaAsN laser as compared with that measured from the InGaAs laser sample. The smaller τ_{esc} will lead to reduced current injection efficiency, as well as a reduction of the modulation bandwidth of the lasers [40]–[42].

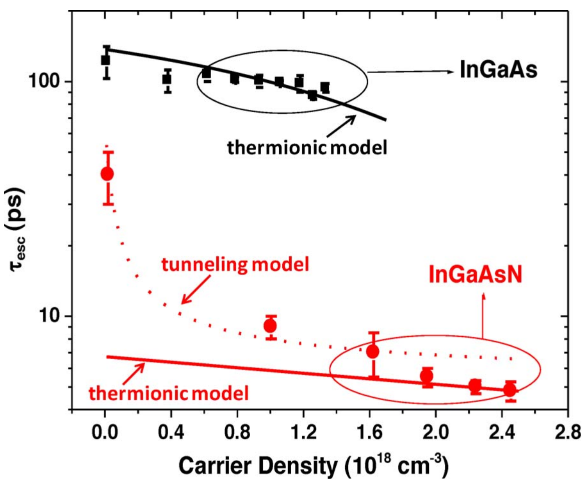

Fig. 4. Experimental (points) and calculated (thermionic processes: solid lines; tunneling: dotted lines) carrier escape times as function of carrier density for InGaAs and InGaAsN lasers.

We performed a thermionic escape time calculation to understand the underlying reason for the decreased τ_{esc} in dilute-nitride laser. Obtaining the relationship between the bias I and carrier density N, the decay time as function of carrier density is plotted in Fig. 4. The relationship between I and N is extracted by measuring the gain spectra and fitting it with an analytical gain model [43].

Treating the carrier escape process via the classical thermionic emission model and considering the state filling effect, the functional dependence of $\tau_{\text{esc}}(N)$ can be calculated using the following analytical equations [33], [44], [45]:

$$\tau_{\text{esc}\_e}(N) = \omega \frac{L_{qw}}{m_{e\_b}} \left(\frac{\pi \hbar^2 m_{e\_w}}{m_{e\_b} k_B T} \right)^{\frac{1}{2}} \frac{\exp\left(\frac{qV_e}{k_B T}\right)}{1 + \exp\left(\frac{E_{fc}(N) - E_{e\_1}}{k_B T}\right)} \tag{1}$$

$$\tau_{\text{esc}\_\text{hh}}(N) = \omega \frac{L_{qw}}{m_{\text{hh}\_b}} \left(\frac{\pi \hbar^2 m_{\text{hh}\_w}}{m_{\text{hh}\_b} k_B T} \right)^{\frac{1}{2}} \frac{\exp\left(\frac{qV_{\text{hh}}}{k_B T}\right)}{1 + \exp\left(\frac{E_{fv}(N) - E_{\text{hh}\_1}}{k_B T}\right)} \tag{2}$$

$$\frac{1}{\tau_{\text{esc}}(N)} = \frac{1}{\tau_{\text{esc}\_e}(N)} + \frac{1}{\tau_{\text{esc}\_\text{hh}}(N)} \tag{3}$$

where ω is a constant related to the escape rate from inside the well to unconfined state in the barrier, in units of $\text{m}^{-1} \cdot \text{kg} \cdot \text{eV}^{-1/2}$, and we assume that ω remains identical for both InGaAs and InGaAsN, L_{qw} is the width of the QW, m_{e_w} (m_{hh_w}) is the effective electron (heavy hole) mass in the well, and m_{e_b} (m_{hh_b}) is the electron (hole) mass of the barrier. qV_e and qV_{hh} are the energy difference between the first confined electron (heavy hole) state and the edge of barrier conduction and valence bands, respectively. $E_{fc}(N)$ $[E_{fv}(N)]$ corresponds to the electron (hole) quasi-Fermi level for confined carriers, and $E_{e\_1}(E_{\text{hh}\_1})$ is the energy level of the first confined level.

Note that, for the case with more than one confined energy level, the escape time is replaced by a summation over all energy levels involved. For the carrier densities of our interest ($< 3 \times 10^{18}$ cm^{-3}), the quasi-Fermi level is far below the second confined level for both electron and holes; thus, the corresponding exponential term in the denominator is much less than 1 and is negligible. Table 1 summarizes all the parameters used in our paper.

The results of the calculation are plotted in Fig. 4, together with the relaxation times determined experimentally. The solid lines are the results for free-carrier thermionic escape, where the difference between InGaAs and InGaAsN lasers in the calculation are only the electron effective mass and band offset ratio. For a value of $\omega = 2.1 \times 10^{-21}$ $\text{m}^{-1} \cdot \text{kg} \cdot \text{eV}^{-1/2}$ chosen, the escape time of one order less is obtained for InGaAsN showing good agreement from other theoretical calculations

TABLE 1

Band parameters used in the simulations of the tunneling and thermionic carrier escape times for both InGaAs QW and InGaAsN QW [42], [43].

	$In_{0.4}Ga_{0.6}As_{0.995}N_{0.005}/GaAs$	$In_{0.4}Ga_{0.6}As/GaAs$
ΔE_c	431 meV	251 meV
ΔE_v	95 meV	177 meV
qV_e	360 meV	177 meV
qV_{hh}	85.6 meV	163.5 meV
$m_{e\ w}$	0.11 m_0	0.047 m_0
$m_{e\ b}$	0.067 m_0	0.067 m_0
$m_{hh\ w}$	0.465 m_0	0.465 m_0
$m_{hh\ b}$	0.51 m_0	0.51 m_0
ω (free carrier)	$2.1\times10^{-21}\ m^{-1}\cdot kg\cdot eV^{-1/2}$	$2.1\times10^{-21}\ m^{-1}\cdot kg\cdot eV^{-1/2}$
ω (exciton)	$5\times10^{-21}\ m^{-1}\cdot kg\cdot eV^{-1/2}$	$5\times10^{-21}\ m^{-1}\cdot kg\cdot eV^{-1/2}$

on the same laser structures reported previously [28]. Notice that, while the calculation gives similar values at higher carrier density, the function trend is off at low carrier density, especially for InGaAsN.

The discrepancy between the measurements of τ_{esc} for InGaAsN laser and the results from the thermionic simulation indicates that there are other mechanisms that dominate the carrier escape at low carrier density [40]–[42]. One such possible carrier escape mechanism at low carrier density is the tunneling phenomena. From the carrier tunneling rate expressions in (4) and (5) [42], one finds that the carrier escape mediated by the tunneling process has a stronger dependence on carrier density, which shows that a faster decay rate with increased carrier density (index of 3/2 in exponential term) would be expected as compared with the thermionic model with exponential index of 1 for electrons and holes, as follows:

$$\tau_{\text{tun\_}e}(N) \sim \exp\left(\frac{4}{3}\frac{\sqrt{2m_e^*}}{e\hbar F(N)}\left(V_e-(E_{fc}(N)-E_{e\_1})\right)^{\frac{3}{2}}\right) \tag{4}$$

$$\tau_{\text{tun\_hh}}(N) \sim \exp\left(\frac{4}{3}\frac{\sqrt{2m_{\text{hh}}^*}}{e\hbar F(N)}\left(V_e-(E_{fv}(N)-E_{\text{hh\_1}})\right)^{\frac{3}{2}}\right). \tag{5}$$

In the above expressions, $F(N)$ is the built-in field resulting from the biasing, which contributes to the decrease in escape time with carrier density. Assuming that the impedance of the laser diode does not change with bias, the built-in field is proportional to the biasing current.

The dotted line in Fig. 4 is the simulation result considering only tunneling in the InGaAsN QW laser. All the parameters used in the fitting are the same as those in Table 1. Note that the thermionic carrier escape rates [42] primarily depends on the conduction- and valence-band offsets for respective QW structures, as well as the corresponding effective masses for both carriers in respective QWs. In our studies, the band offsets and corresponding effective masses for InGaAs QW and InGaAsN QW were taken from references [42] and [43]. In our paper, the structures consist of InGaAs QW and InGaAsN QW with direct GaAs barriers followed by tensile GaAsP barriers for strain compensation purposes. Thus, the direct heterostructures studied here consist of InGaAs(N)/GaAs and InGaAsN/GaAs interfaces. The agreement at lower carrier densities for InGaAsN QW is remarkable and explains the steep decay of τ_{esc} clearly showing the dominance of carrier escape out of the well through tunneling at low-carrier-density regime. As carrier density increases in InGaAsN QW, both thermionic escape and tunneling become important. However, at the very high carrier density in the InGaAsN QW, the carrier escape in InGaAsN QW appears to be sufficiently described by the thermionic carrier escape model.

The analysis and experimental results of this paper shows that the thermionic carrier escape model taking into consideration the hole leakage provides good agreement with the experimental data for InGaAsN QW lasers. These results agree well with the previously reported studies on the possibility of hole carrier leakage in InGaAsN QWs [33], [42], [46]–[48]. The use of GaAsP direct barriers with larger band offset to surround the InGaAsN QW had resulted in a reduction in the threshold current density and an increase in the differential quantum efficiency for strain-compensated dilute-nitride lasers [13], [42]. In addition, recent theoretical works by Healy and O'Reilly [16] had also shown that the implementation of GaAsP barriers leads to improved hole confinement in the InGaAsN QW. However, it is important to note that other possible leakage mechanisms in InGaAsN QW that can lead to thermionic carrier escape processes. Recent findings by Chamings *et al.* have also suggested the possibility of carrier leakage process via defect states recombination in barrier regions in dilute-nitride QW structure [49].

Note that the results for the InGaAs QW lasers indicate that the carrier escape processes appear to be dominated by the thermionic carrier escape, as supported by the good agreement between the theoretical model and experimental results for InGaAs QW (see Fig. 4). Furthermore, note that the thermionic carrier escape rate appears to be an order of magnitude lower than that of InGaAsN QW.

In the analysis of the current injection efficiency and modulation bandwidth in QW lasers, both the carrier escape time (τ_{esc}) and carrier capture time (τ_{cap}) are of importance. Generally, it is not just the value of carrier escape time but the ratio of capture and escape time constant $(R = \tau_{cap}/\tau_{esc})$ that determines the modulation response and current injection efficiency in QW laser. Note that the τ_{cap} is the sum of quantum capture time τ_{cap_qw} and the transport time from the edge of barrier to the QW, i.e., τ_{tr}. The rise time in our pump–probe data indicates that the quantum capture time τ_{cap_qw} is less than 1 ps for both InGaAsN and InGaAs QWs. In our studies, τ_{tr} was calculated by using the approach in reference [32], and τ_{tr} was found as constant $\sim$5.3 ps in both InGaAsN and InGaAs lasers. In addition, we also determined the transport time as $\sim$10 ps from TRPL rise time. Thus, we conclude that transport time is the dominant contribution to τ_{cap} in both lasers and that the introduction of nitrogen does not affect τ_{cap} significantly. This finding is consistent with general knowledge on the physics of QW lasers. The measurements of the distinct differences in thermionic carrier escape processes in InGaAs/GaAs QW and InGaAsN/GaAs QW lasers point out to the importance of taking into account the carrier escape processes in QW LEDs and lasers, and the finding and method described here are useful for providing improved understanding of the characteristics of electrically injected other QW LEDs and lasers operating at high current density including for providing insight into the efficiency-droop phenomenon in InGaN-based QW devices [50]–[56].

4. Summary

We have independently measured carrier escape times τ_{esc} for both InGaAsN and InGaAs QWs lasers. From our experiments, we found that τ_{esc} in InGaAsN QW laser is almost an order of magnitude lower in comparison with that measured in InGaAs QW laser. We show that the dependence of τ_{esc} for InGaAsN QW laser in the low carrier density regime can only be explained by taking into account the carrier escape process by tunneling phenomena. The tunneling carrier escape mechanism is most important at low carrier densities in InGaAsN QW due to the smaller band offset ratio, particularly for the valence-band offset. Thermionic carrier escape process is dominant for InGaAsN QW laser operating at high-carrier-density regime. In contrast, the carrier escape process in InGaAs QW laser can be well explained only with the thermionic carrier escape model for both low and high carrier density regimes. Together with TRPL measurements, the ratio of τ_{cap}/τ_{esc} of InGaAsN laser device was found to have strong carrier density dependent, while minimal-carrier-density-dependent τ_{cap}/τ_{esc} was observed for InGaAs QW lasers. The finding shows the importance of taking into consideration the effect of carrier escape processes on current injection efficiency in QW lasers or LEDs operating at high current density, which clearly indicates that the current injection efficiency needs to be accounted for in the analysis of internal quantum efficiency and laser characteristics in QW devices [42]. In addition, these results provide improved understanding on the device physics of current injection efficiency in electrically injected QW devices, which is an imperative parameter for addressing solutions to achieve low-threshold lasers operating at high temperature and suppress efficiency-droop phenomenon in III–V or III-Nitride QW LEDs.

References

[1] D. A. Livshits, A. Y. Egorov, and H. Riechert, "8 W continuous wave operation of InGaAsN lasers at 1.3 μm," *Electron. Lett.*, vol. 36, no. 16, pp. 1381–1382, Aug. 2000.

[2] S. R. Bank, M. A. Wistey, H. B. Yuen, L. L. Goddard, W. Ha, and J. S. Harris, Jr., "Low-threshold CW GaInNAsSb/GaAs laser at 1.49μm," *Electron. Lett.*, vol. 39, no. 20, pp. 1445–1446, Oct. 2003.

[3] S. R. Bank, H. B. Yuen, M. A. Wistey, V. Lordi, H. P. Bae, and J. S. Harris, "Effects of growth temperature on the structural and optical properties of 1.55 μm GaInNAsSb quantum wells grown on GaAs," *Appl. Phys. Lett.*, vol. 87, no. 2, pp. 021908-1–021908-3, Jul. 2005.

[4] N. Tansu, J. Y. Yeh, and L. J. Mawst, "Physics and characteristics of 1200-nm InGaAs and 1300–1400 nm InGaAsN quantum-well lasers by metalorganic chemical vapor deposition," *J. Phys., Condens. Matter Phys.*, vol. 16, no. 31, pp. S3277–S3318, Aug. 2004.

[5] J. Lyytikainen, J. Rautiainen, L. Toikkanen, A. Sirbu, A. Mereuta, A. Caliman, E. Kapon, and O. G. Okhotnikov, "1.3-μm optically-pumped semiconductor disk laser by wafer fusion," *Opt. Exp.*, vol. 17, no. 11, pp. 9047–9052, May 2009.

[6] D. Bisping, D. Pucicki, M. Fischer, J. Koeth, C. Zimmermann, P. Weinmann, S. Hofling, M. Kamp, and A. Forchel, "GaInNAs-based high-power and tapered laser diodes for pumping applications," *IEEE J. Sel. Topics Quantum Electron.*, vol. 15, no. 3, pp. 968–972, May/Jun. 2009.

[7] Y. Onishi, N. Saga, K. Koyama, H. Doi, T. Ishizuka, T. Yamada, K. Fujii, H. Mori, J. Hashimoto, M. Shimazu, A. Yamaguchi, and T. Katsuyama, "Long-wavelength GaInNAs vertical-cavity surface-emitting laser with buried tunnel junction," *IEEE J. Sel. Topics Quantum Electron.*, vol. 15, no. 3, pp. 838–843, May/Jun. 2009.

[8] H. P. D. Yang, C. T. Shih, S. M. Yang, and T. D. Lee, "High-power broad-area InGaNAs/GaAs quantum-well lasers in the 1200 nm range," *Microelectron. Reliab.*, vol. 50, no. 5, pp. 722–725, May 2010.

[9] S. M. Wang, G. Adolfsson, H. Zhao, Y. X. Song, M. Sadeghi, J. Gustavsson, P. Modh, A. Haglund, P. Westbergh, and A. Larsson, "Growth of dilute nitrides and 1.3μm edge emitting lasers on GaAs by MBE," *Phys. Stat. Sol. (B)*, vol. 248, no. 5, pp. 1207–1211, May 2011.

[10] S. R. Bank, L. L. Goddard, M. A. Wistey, H. B. Yuen, and J. S. Harris, "On the temperature sensitivity of 1.5-μm GaInNAsSb lasers," *IEEE J. Sel. Topics Quantum Electron.*, vol. 11, no. 5, pp. 1089–1098, Sep./Oct. 2005.

[11] L. L. Goddard, S. R. Bank, M. A. Wistey, H. B. Yuen, Z. Rao, and J. S. Harris, "Recombination, gain, band structure, efficiency, and reliability of 1.5-μm GaInNAsSb/GaAs lasers," *J. Appl. Phys.*, vol. 97, no. 8, pp. 083101-1–083101-15, Apr. 2005.

[12] R. Fehse, S. Tomic, A. R. Adams, S. J. Sweeney, E. P. O'Reilly, A. Andreev, and H. Riechert, "A quantitative study of radiative, auger, and defect related recombination processes in 1.3-μm GaInNAs-based quantum well lasers," *IEEE J. Sel. Topics Quantum Electron.*, vol. 8, no. 4, pp. 801–810, Jul./Aug. 2002.

[13] N. Tansu, J. Y. Yeh, and L. J. Mawst, "Experimental evidence of carrier leakage in InGaAsN quantum well lasers," *Appl. Phys. Lett.*, vol. 83, no. 11, pp. 2112–2114, Sep. 2003.

[14] G. Adolfsson, S. M. Wang, M. Sadeghi, J. Bengtsson, A. Larsson, J. J. Lim, V. Vilokkinen, and P. Melanen, "Effects of lateral diffusion on the temperature sensitivity of the threshold current for 1.3-μm double quantum-well GaInNAs–GaAs lasers," *IEEE J. Quantum Electron.*, vol. 44, no. 7/8, pp. 607–616, Jul./Aug. 2008.

[15] J. W. Ferguson, P. Blood, P. M. Smowton, H. Bae, T. Sarmiento, J. S. Harris, N. Tansu, and L. J. Mawst, "Optical gain in GaInNAs and GaInNAsSb quantum wells," *IEEE J. Quantum Electron.*, vol. 47, no. 6, pp. 870–877, Jun. 2011.

[16] S. B. Healy and E. P. O'Reilly, "Influence of electrostatic confinement on optical gain in GaInNAs quantum-well lasers," *IEEE J. Quantum Electron.*, vol. 42, no. 5/6, pp. 608–615, May/Jun. 2006.

[17] S. Tomic and E. P. O'Reilly, "Influence of confinement energy and band anticrossing effect on the electron effective mass in $Ga_{1-y}In_yN_xAs_{1-x}$ quantum wells," *Phys. Rev. B*, vol. 71, no. 23, pp. 233301-1–233301-4, Jun. 2005.

[18] M. M. Bajo, A. Hierro, J. M. Ulloa, J. Miguel-Sanchez, A. Guzman, B. Damilano, M. Hugues, M. Al-Khalfioui, J. Y. Duboz, and J. Massies, "Current spreading efficiency and Fermi level pinning in GaInNAs–GaAs quantum-well laser diodes," *IEEE J. Quantum Electron.*, vol. 46, no. 7, pp. 1058–1065, Jul. 2010.

[19] D. J. Palmer, P. M. Smowton, P. Blood, J. Y. Yeh, L. J. Mawst, and N. Tansu, "Effect of nitrogen on gain and efficiency in InGaAsN quantum well lasers," *Appl. Phys. Lett.*, vol. 86, no. 7, pp. 071121-1–071121-3, Feb. 2005.

[20] H. Carrere, X. Marie, J. Barrau, and T. Amand, "Comparison of the optical gain of InGaAsN quantum-well lasers with GaAs or GaAsP barriers," *Appl. Phys. Lett.*, vol. 86, no. 7, pp. 071116-1–071116-3, Feb. 2005.

[21] A. Thranhardt, I. Kuznetsova, C. Schlichenmaier, S. W. Koch, L. Shterengas, G. Belenky, J. Y. Yeh, L. J. Mawst, N. Tansu, J. Hader, J. V. Moloney, and W. W. Chow, "Nitrogen incorporation effects on gain properties in GaInNAs lasers: Experiment and theory," *Appl. Phys. Lett.*, vol. 86, no. 20, pp. 201117-1–201117-3, May 2005.

[22] C. Schlichenmaier, A. Thranhardt, T. Meier, S. W. Koch, W. W. Chow, J. Hader, and J. V. Moloney, "Gain and carrier losses of (GaIn)(NAs) heterostructures in the 1300–1550 nm range," *Appl. Phys. Lett.*, vol. 87, no. 26, pp. 261109-1–261109-3, Dec. 2005.

[23] S. D. Wu, Y. G. Cao, S. Tomic, and F. Ishikawa, "The optical gain and radiative current density of GaInNAs/GaAs/AlGaAs separate confinement heterostructure quantum well lasers," *J. Appl. Phys.*, vol. 107, no. 1, pp. 013107-1–013107-6, Jan. 2010.

[24] D. Gollub, S. Moses, and A. Forchel, "1.3 μm double quantum well GaInNAs distributed feedback laser diode with 13. 8 GHz small signal modulation bandwidth," *Electron. Lett.*, vol. 40, no. 19, pp. 1181–1182, Sep. 2004.

[25] J. S. Gustavsson, Y. Q. Wei, M. Sadeghi, S. M. Wang, and A. Larsson, "10 Gbit/s modulation of 1.3 μm GaInNAs lasers up to 110 °C," *Electron. Lett.*, vol. 42, no. 16, pp. 925–926, Aug. 2006.

[26] W. Shan, W. Walukiewicz, J. W. Ager, E. E. Haller, J. F. Geisz, D. J. Friedman, J. M. Olson, and S. R. Kurtz, "Band anticrossing in GaInNAs alloys," *Phys. Rev. Lett.*, vol. 82, no. 6, pp. 1221–1224, Feb. 1999.

[27] J. C. L. Yong, J. M. Rorison, M. Othman, H. D. Sun, M. D. Dawson, and K. A. Williams, "Simulation of gain and modulation bandwidths of 1300 nm RWG InGaAsN lasers," *Proc. Inst. Elect. Eng.—Optoelectron.*, vol. 150, no. 1, pp. 80–82, Feb. 2003.

[28] S. C. Kan, D. Vassilovski, T. C. Wu, and K. Y. Lau, "Quantum capture and escape in quantum-well lasers—Implications on direct modulation bandwidth limitations," *IEEE Photon. Technol. Lett.*, vol. 4, no. 5, pp. 428–431, May 1992.

[29] R. Nagarajan, M. Ishikawa, T. Fukushima, R. S. Geels, and J. E. Bowers, "High-speed quantum well lasers and carrier transport effects," *IEEE J. Quantum Electron.*, vol. 28, no. 10, pp. 1990–2008, Oct. 1992.

[30] R. Nagarajan and J. E. Bowers, "Effects of carrier transport on injection efficiency and wavelength chirping in quantum-well lasers," *IEEE J. Quantum Electron.*, vol. 29, no. 6, pp. 1601–1608, Jun. 1993.

[31] Y. Q. Wei, J. S. Gustavsson, A. Haglund, P. Modh, M. Sadeghi, S. M. Wang, and A. Larsson, "High-frequency modulation and bandwidth limitations of GaInNAs double-quantum-well lasers," *Appl. Phys. Lett.*, vol. 88, no. 5, pp. 051103-1–051103-3, Jan. 2006.

[32] O. Anton, L. Xu, D. Patel, C. S. Menoni, J. Y. Yeh, T. T. Van Roy, L. J. Mawst, and N. Tansu, "The intrinsic frequency response of 1.3-μm InGaAsN Lasers in the range $T = 10\ °C-80\ °C$," *IEEE Photon. Technol. Lett.*, vol. 18, no. 16, pp. 1774–1776, Jul./Aug. 2006.

[33] N. Tansu and L. J. Mawst, "The role of hole-leakage in 1300-nm InGaAsN quantum well lasers," *Appl. Phys. Lett.*, vol. 82, no. 10, pp. 1500–1502, Mar. 2003.

[34] N. Tansu, N. J. Kirsch, and L. J. Mawst, "Low-threshold-current-density 1300-nm dilute-nitride quantum well lasers," *Appl. Phys. Lett.*, vol. 81, no. 14, pp. 2523–2525, Sep. 2002.

[35] D. Stehr, M. Wagner, H. Schneider, M. Helm, A. M. Andrews, T. Roch, and G. Strasser, "Two-color pump–probe studies of intra miniband relaxation in doped GaAs/AlGaAs superlattices," *Appl. Phys. Lett.*, vol. 92, no. 5, pp. 051104-1–051104-3, Feb. 2008.

[36] K. L. Silverman, R. P. Mirin, and S. T. Cundiff, "Lateral coupling of $In_xGa_{1-x}As$/GaAs quantum dots investigated using differential transmission spectroscopy," *Phys. Rev. B, Condens. Matter Mater Phys.*, vol. 70, no. 20, pp. 205310-1–205310-5, Nov. 2004.

[37] J. Hamazaki, H. Kunugita, K. Ema, A. Kikuchi, and K. Kishino, "Intersubband relaxation dynamics in GaN/AlN multiple quantum wells studied by two-color pump–probe experiments," *Phys. Rev. B, Condens. Matter Mater. Phys.*, vol. 71, no. 16, pp. 165334-1–165334-5, Apr. 2005.

[38] L. Xu, D. Patel, C. S. Menoni, J. Y. Yeh, L. J. Mawst, and N. Tansu, "Optical determination of electron effective-mass of strain compensated $In_{0.4}Ga_{0.6}As_{0.995}N_{0.005}/GaAs$ single quantum well," *Appl. Phys. Lett.*, vol. 89, no. 17, pp. 171112-1–171112-3, Oct. 2006.

[39] J. Y. Yeh, N. Tansu, and L. J. Mawst, "Temperature-sensitivity analysis of 1360-nm dilute-nitride quantum-well lasers," *IEEE Photon. Technol. Lett.*, vol. 16, no. 3, pp. 741–743, Mar. 2004.

[40] C. Y. Tsai, C. Y. Tsai, Y. H. Lo, R. M. Spencer, and L. F. Eastman, "Nonlinear gain coefficients in semiconductor quantum-well lasers—Effects of carrier diffusion, capture, and escape," *IEEE J. Sel. Topics Quantum Electron.*, vol. 1, no. 2, pp. 316–330, Jun. 1995.

[41] G. Vincent, A. Chantre, and D. Bois, "Electric-field effect on the thermal emission of traps in semiconductor junctions," *J. Appl. Phys.*, vol. 50, no. 8, pp. 5484–5487, Aug. 1979.

[42] N. Tansu and L. J. Mawst, "Current injection efficiency of 1300-nm InGaAsN quantum-well lasers," *J. Appl. Phys.*, vol. 97, no. 5, pp. 054502-1–054502-18, Mar. 2005.

[43] S. L. Chuang, *Physics of Photonic Devices,* 2nd ed. New York: Wiley, 2009.

[44] B. Romero, J. Arias, I. Esquivias, and M. Cada, "Simple model for calculating the ratio of the carrier capture and escape times in quantum-well lasers," *Appl. Phys. Lett.*, vol. 76, no. 12, pp. 1504–1506, Mar. 2000.

[45] H. Schneider and K. V. Klitzing, "Thermionic emission and Gaussian transport of holes in GaAs/$Al_xGa_{1-x}As$ multiple-quantum-well structure," *Phys. Rev. B, Condens. Matter Mater. Phys.*, vol. 38, no. 9, pp. 6160–6165, Sep. 1988.

[46] M. Hugues, B. Damilano, J.-Y. Duboz, and J. Massies, "Exciton dissociation and hole escape in the thermal photoluminescence quenching of (Ga,In)(N,As) quantum wells," *Phys. Rev. B, Condens. Matter Mater. Phys.*, vol. 75, no. 11, pp. 115337-1–115337-5, Mar. 2007.

[47] A. Albo, G. Bahir, and D. Fekete, "Improved hole confinement in GaInAsN–GaAsSbN thin double-layer quantum-well structure for telecom-wavelength lasers," *J. Appl. Phys.*, vol. 108, no. 9, pp. 093 116-1–093 116-6, Nov. 2010.

[48] J. Y. Yeh, N. Tansu, and L. J. Mawst, "The role of carrier transport on the current injection efficiency of InGaAsN quantum-well lasers," *IEEE Photon. Technol. Lett.*, vol. 17, no. 9, pp. 1779–1881, Sep. 2005.

[49] J. Chamings, S. Ahmed, A. R. Adams, S. J. Sweeney, V. A. Odnoblyudov, C. W. Tu, B. Kunert, and W. Stolz, "Band anti-crossing and carrier recombination in dilute nitride phosphide based lasers and light emitting diodes," *Phys. Stat. Sol. (B)*, vol. 246, no. 3, pp. 527–531, Mar. 2009.

[50] V. S. Sizov, V. V. Neploh, A. F. Tsatsulnikov, A. V. Sakharov, W. V. Lundin, E. E. Zavarin, A. E. Nikolaev, A. M. Mintairov, and J. L. Merz, "Study of tunneling transport of carriers in structures with an InGaN/GaN active region," *Semiconductors*, vol. 44, no. 12, pp. 1567–1575, Dec. 2010.

[51] M. F. Schubert, J. Xu, J. K. Kim, E. F. Schubert, M. H. Kim, S. Yoon, S. M. Lee, C. Sone, T. Sakong, and Y. Park, "Polarization-matched GaInN/AlGaInN multi-quantum-well light-emitting diodes with reduced efficiency droop," *Appl. Phys. Lett.*, vol. 93, no. 4, pp. 041102-1–041102-3, Jul. 2008.

[52] H. Zhao, G. Liu, R. A. Arif, and N. Tansu, "Current injection efficiency quenching leading to efficiency droop in InGaN quantum well light-emitting diodes," *Solid State Electron.*, vol. 54, no. 10, pp. 1119–1124, Oct. 2010.

[53] X. Ni, X. Li, J. Lee, S. Liu, V. Avrutin, A. Matulionis, U. Ozgur, and H. Morkoc, "Pivotal role of ballistic and quasi-ballistic electrons on LED efficiency," *Superlattices Microstruct.*, vol. 48, no. 2, pp. 133–153, Aug. 2010.

[54] U. Ozgur, H. Y. Liu, X. Li, X. F. Ni, and H. Morkoc, "GaN-based light-emitting diodes: Efficiency at high injection levels," *Proc. IEEE*, vol. 98, no. 7, pp. 1180–1196, Jul. 2010.

[55] J. Piprek, "Efficiency droop in nitride-based light-emitting diodes," *Phys. Stat. Sol. (A)*, vol. 207, no. 10, pp. 2217–2225, Oct. 2010.

[56] S. Choi, H. J. Kim, S.-S. Kim, J. Liu, J. Kim, J.-H. Ryou, R. D. Dupuis, A. M. Fischer, and F. A. Ponce, "Improvement of peak quantum efficiency and efficiency droop in III-nitride visible light-emitting diodes with an InAlN electron-blocking layer," *Appl. Phys. Lett.*, vol. 96, no. 22, pp. 221105-1–221105-3, May 2010.